Journal of Applied Polymer Science

REVIEW

Polyaniline Nanocomposites with Negative Permittivity

Hongbo Gu,[1] Jiang Guo,[1] Suying Wei,[2] Zhanhu Guo[1]

[1]Integrated Composites Lab, Dan F. Smith Department of Chemical Engineering, Lamar University, Beaumont, Texas 77710

[2]Department of Chemistry and Biochemistry, Lamar University, Beaumont, Texas 77710

Correspondence to: Z. Guo (E-mail: zhanhu.guo@lamar.edu)

ABSTRACT: In this review, the fundamentals of negative permittivity are critically discussed. Current research on polyaniline and its nanocomposites with negative permittivity are presented in detail. The reasons why these unique materials show negative permittivity are analyzed. This knowledge will be useful for future metacomposite design and manufacturing. These polymeric materials with negative permittivity are envisioned to create next-generation left-hand media for cloaking, subwavelength imaging, stealth, and invisibility applications. © 2013 Wiley Periodicals, Inc. J. Appl. Polym. Sci. 130: 2238–2244, 2013

KEYWORDS: composites; conducting polymers; dielectric properties; magnetization and magnetic properties; nanostructured polymers

Received 12 March 2013; accepted 18 April 2013; Published online 28 June 2013

DOI: 10.1002/app.39420

INTRODUCTION

In recent years, materials with both negative permittivity and permeability (called a *negative refractive index*) at a given frequency of radiation are called *metamaterials*.[1,2] Metamaterials are not obtainable in nature[3] and instead are artificially constructed with special structures and unique electromagnetic properties. In the metamaterials, the triad of vectors, including the macroscopic electric field (**E**), magnetic field (**H**), and wave vector (**k**), is left-handed because the Poynting vector determined from **E**×**H** is opposite to the wave vector **k**.[4] Thus, these special materials firstly proposed by Veselago in 1968 are called *left-handed media*.[5] These materials have gained more attention in the last decade because of their unique negative refractive index, permittivity, and/or permeability for cloaking, subwavelength imaging, and invisibility applications.[6,7]

Negative permittivity is one of the unique characteristic properties of metamaterials.[8] Recently, the term *metacomposites* was introduced to describe nanocomposites with a unique negative permittivity; they have potential promising applications for superlenses, wave filters, remote aerospace applications, and superconductors.[9,10] This unique negative permittivity has been reported in various nanocomposites, including polyaniline (PANI),[11] polypyrrole,[12,13] carbon nanofibers (CNFs)/elastomer nanocomposites,[14] epoxy,[15] graphene,[16] and graphene nanocomposites.[17] The negative permittivity observed in conductive polymer nanocomposites can be easily tuned by changing the particle loading levels, the ratio of oxidant to the monomer, and nanofiller morphologies.[9,10] The negative permittivity in the two-dimensional graphene and graphene nanocomposites arises from the unique electronic energy dispersions (also called *surface plasmons*).[16,17]

PANI is distinct from other conjugated polymer systems because of the presence of alternative amine and imine groups in the polymer backbone.[18] The amine groups (NH) in the polymer chain give PANI a very high chemical flexibility in the system. For example, PANI has been reported as a coupling agent to improve the compatibility between the nanofillers and the hosting epoxy matrix.[18–21] PANI is formed by the overlap of nitrogen p_z orbitals. The hetero atom (nitrogen atom) contributes significantly to the π-band formation and conduction mechanism, which is different from other conductive polymers, such as polypyrrole, polythiophenes, and polyfuran.[22,23] It has received special attention because of its intriguing properties, including its easy synthesis, light weight, low cost, good environmental stability, three distinct oxidation states with different colors, simple doping/dedoping process, and high pseudocapacitance.[24–26] PANI has been widely applied in many fields, including supercapacitors,[25] anticorrosion,[27] hole injection layers,[28] electrochromic materials,[29] electromagnetic interference shielding,[22] and environmental remediation.[30]

Although some reviews regarding conductive polymers have been reported,[31–33] the negative permittivity of PANI and its nanocomposites have not yet been reviewed. In this review, the fundamentals of negative permittivity are critically examined, and the research reports on PANI and its nanocomposites with negative permittivity are discussed in detail.

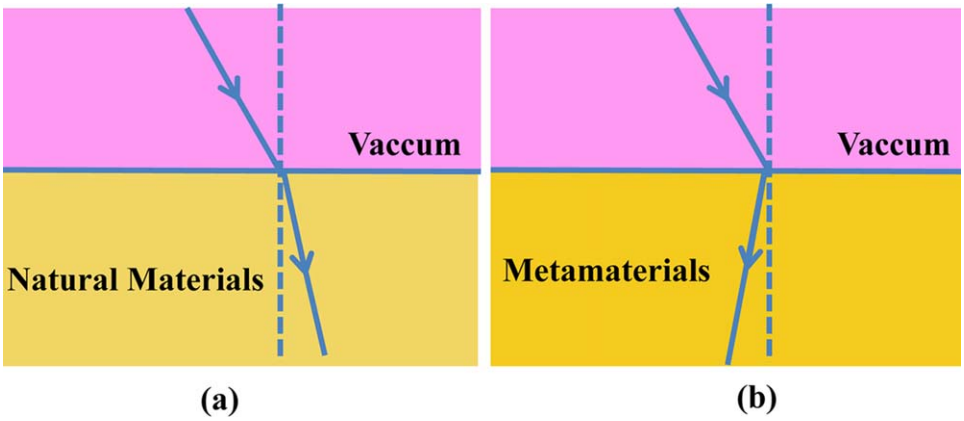

Figure 1. Schematic of (a) the positive refractive index in natural materials and (b) negative refractive index in metamaterials.[Color figure can be viewed in the online issue, which is available at wileyonlinelibrary.com.]

FUNDAMENTALS

Generally, in natural materials with positive refractive index, the light gets bent in the direction of propagation when it crosses from a vacuum to natural materials [Figure 1(a)]. However, in metamaterials, the light will become backward for the propagation because of the occurrence of negative refraction [Figure 1(b)]. The dielectric properties describe the ability that an electrical medium can be polarized by an applied electric field.[34] When a dielectric medium is placed in an electric field, electrical charges shift from their average equilibrium positions and cause dielectric polarization (displacement). Frequency-dependent dielectric properties reflect the fact that the polarization of these materials does not respond to an applied electric field instantaneously; this is related to the polarizability of the atoms and molecules in an electrical medium. The applied electric field causes the charge separation of the positively charged nuclei and the negatively charged electrons in the atoms and molecules to induce a dipole moment.[35] In the metals, the mass of the negative charges (electrons) is assumed to be much smaller than that of the positive charges (ion cores in the metal), which means that only the motion of the electrons contributes to the polarization in the medium. Thus, the motion of the nuclei is negligible because of their comparatively large mass. The Lorentz force (**F**) on the electron is expressed as eq. (1):

$$\mathbf{F}=-e(\mathbf{E}+\boldsymbol{\upsilon}\times\mathbf{H}) \tag{1}$$

where υ is the velocity of the electrons and e is the electron charge. The electron in an atom or molecule is assumed to be bound to the equilibrium position via an elastic restoring force. Therefore, the equation of electron motion becomes eq. (2):

$$m\ddot{\mathbf{r}}+m\gamma\dot{\mathbf{r}}+m\omega_0^2\mathbf{r}=-e\mathbf{E}_0\exp(-i\omega t) \tag{2}$$

where $\mathbf{r}$ is the displacement vector; $\ddot{\mathbf{r}}$ is the second derivative with respect to t; $\dot{\mathbf{r}}$ is the first derivative with respect to t; ω_0 is the resonance angular frequency, which characterizes the harmonic potential trapping of the electron to the equilibrium position; m is the mass of the electron; ω is the angular frequency; $m\gamma$ is the phenomenological damping force constant due to all of the inelastic processes and is inversely proportional to the electron mean free path; γ is the dissipation parameter; and t is the time. The displacement vector $\mathbf{r}$ of the electron under an alternative $\boldsymbol{E}$ can be obtained with a trial solution: $\mathbf{r}=\mathbf{r_0}\exp(-i\omega t)$ and expressed as eq. (3):[35]

$$r_0=\frac{e\mathrm{E}/m}{\omega(\omega+i\gamma)} \tag{3}$$

After the magnetic contribution to $\boldsymbol{F}$ is neglected, the equation of the motion for an electron in a time harmonic $\boldsymbol{E}$ with ω is expressed as eq. (4):[35]

$$mr+m\gamma r=-eE\exp(-i\omega t) \tag{4}$$

The wavelength of the radiation is assumed to be large compared to the travelled distance by the electrons, and thus, the electrons can effectively move along a spatially uniform field. Therefore, the dipole moment of each electron is $p=-e\mathbf{r}$, and the polarization ($\boldsymbol{P}$), defined as the dipole moment per unit volume, can be expressed as eq. (5):[35]

$$P=(\varepsilon-1)\varepsilon_0E=-Ner=-\frac{Ne^2/mE}{\omega(\omega+i\gamma)} \tag{5}$$

where ε is the relative dielectric permittivity, ε_0 is the vacuum permittivity, and N is the charge-carrier density. The relative complex dielectric permittivity is expressed as eq. (6) and is also called the Drude model:[35,36]

$$\begin{aligned}\varepsilon(\omega)&=1-\frac{Ne^2/(\varepsilon_0 m)}{\omega(\omega+i\gamma)}=1-\frac{\omega_p^2}{\omega(\omega+i\gamma)}\\&=\left(1-\frac{\omega_p^2}{\omega^2+\gamma^2}\right)+\left[\frac{\omega_p^2\gamma}{\omega(\omega^2+\gamma^2)}\right]i\end{aligned} \tag{6}$$

where $\omega_p\equiv(Ne^2/\varepsilon_0 m)^{1/2}=(4\pi Ne^2/m^\star)$ is the plasma frequency and $m^\star$ is the effective mass of the electron.[37] From eq. (6), the real part of the permittivity [expressed as $1-\frac{\omega_p^2}{\omega^2+\gamma^2}$ is negative for $\omega<\omega_p$ [when the dissipation (γ) is negligible, which means

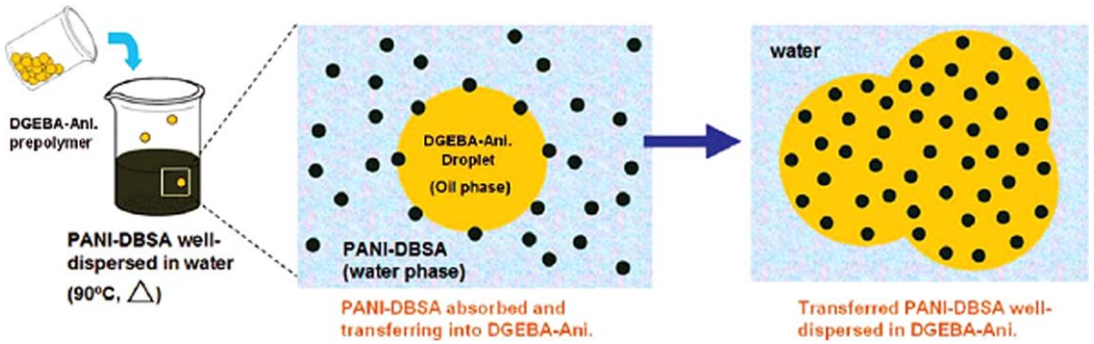

Figure 2. Schematic of the absorption–transferring process. Diglycidyl ether of bisphenol A (DGEBA) represents the epoxy resin DER 331. (Reprinted with permission from ref. 15. Copyright 2008 ACS Publications.) [Color figure can be viewed in the online issue, which is available at wileyonlinelibrary.com.]

that when the frequencies are lower than ω_p, the charges can move quickly to shield the interior of the medium from the electromagnetic radiation. When the frequency is larger than ω_p, the medium behaves as an ordinary dielectric medium.[4] This model has also been reported to be consistent with the results obtained in metallic PANI polymers.[38] Lee et al.[38] used the Drude model to describe a highly conductive PANI–camphorsulfonic acid prepared by self-stabilized dispersion polymerization. The parameter ω_p obtained from the Drude model was reasonable and consistent with the experimental results.

PANI with Negative Permittivity

Conjugated PANI has three different structures, including the fully reduced form, leucoemeraldine; the half-oxidized form, emeraldine (EB); and the fully oxidized form, pernigraniline.[39,40] The conductivity of PANI is strongly dependent on the doping degree, type of dopants, molecular weight, percentage of crystallinity and interchain separation, oxidation level, and molecular arrangement.[41] Generally, the only electrically conductive form is the protonated or doped EB form, and the leucoemeraldine form and pernigraniline form are mainly insulting in nature.[42] The protonation or doping of the EB form can make the electronic structure of PANI chains turn into a polaronic lattice; this results in electric conduction.[43] Mostly, the negative permittivity is observed in the EB salt form PANI (the doped EB form) because of the formation of a continuous conductive network in the PANI polymer chain.[15] It was reported that the dielectric properties correspond to the intrinsic metallic nature of PANI, such as its conductivity and charge delocalization, and this leads to the polarization of the polymer structures.[44] The intrinsic metallic nature of PANI arises from strong interchain interaction in the disordered region, where the interchain interaction is strong enough to allow the charges to be delocalized in three dimensions;[45] this leads to a negative permittivity. The conductive PANI in a metallic state has remarkable frequency-dependent conductivity; this means that the dielectric properties have a strong effect on the conductivity of PANI.[46] The interchain interaction of PANI is an important factor affecting its conductivity.[47] Even though the conductivity can be improved with an increase in the crystallinity, the conductive PANI remains considerably disordered. However, in the crystalline regions, including regions of well-ordered polymer chains (called *metallic islands*), the interchain interaction is strong enough to allow the charge carriers to be delocalized among the crystalline regions, that is, within the disordered regions.[45] Each metallic island in the polymers represents crystalline domains with delocalized electrons embedded in amorphous PANI. Meanwhile, the doped acid can affect the permittivity of PANI. Epstein and coworkers[45,46,48] reported a large negative permittivity in the microwave frequency range for camphorsulfonic acid doped PANI prepared in *m*-cresol. Gu and coworkers[11,49] reported that *p*-toluene sulfonic acid doped PANI exhibited a negative permittivity; however, phosphoric acid (H_3PO_4) doped PANI showed a huge positive permittivity.

Phang et al.[50] reported PANI with a negative permittivity for microwave absorbing and shielding applications. The effects of different parameters, including the doping levels, oxidant ratio, and solvent, on the negative permittivity and microwave absorbing and shielding were systematically investigated. Normally, the electromagnetic absorption behavior of the materials is critically dependent on the permittivity and permeability. However, for doped PANI, this behavior was only related to the permittivity because of the nonmagnetic nature of PANI. The negative permittivity and high conductivity indicated that a more disordered motion of the charge carriers along the backbone of the PANI polymer led to improved microwave behavior in PANI. Zhang et al.[51] synthesized PANI nanofibers with an interfacial polymerization method under different conditions, such as the interfacial area, polymerization time, concentration ratio, and scale ratio. The negative real permittivity (ε') was obtained in all of the samples prepared by the interfacial polymerization method; this indicated the intrinsic metallic state of the synthesized PANI nanofibers. They also investigated the permittivity of the PANI nanoparticles synthesized by a sonication method and a polymeric acid [poly(2-acrylamido-2-methyl-1-propanesulfonic acid)] doping method for comparison. Interestingly, the positive ε' and a negative imaginary permittivity (ε'') were observed at a low frequency ($<10^3$ Hz) in the polymeric acid doped PANI; when the frequency was increased to higher than 10^3 Hz, ε' became negative, and ε'' switched to positive. For the PANI nanoparticles synthesized by a sonication method, a negative ε' was obtained, but it was lower than that of the PANI fibers synthesized by the interfacial polymerization method.

PANI Nanocomposites with a Negative Permittivity

The incorporation of nanofillers in a hosting PANI matrix to form nanocomposites can provide PANI with interesting functionalities, such as a higher electrical conductivity through the introduction of Au or Ag noble metals,[52] enhanced microwave absorption properties with TiO_2 nanoparticles,[53] and other unique magnetic, optical, and catalytic properties.[9] A negative permittivity can also be obtained in PANI nanocomposites with different nanofillers. Liu et al.[15] fabricated the nanopolyaniline/epoxy hybrids with an absorption–transferring process (Figure 2), in which the PANI nanoparticles were absorbed on the surface of the epoxy droplet and then transferred into the whole droplet. The observed huge negative dielectric constant (-10^4 to -10^5) in the prepared hybrids was due to the continuous conducting pathway formed by PANI and the delocalized charges on a macroscopic scale. However, a positive dielectric constant (10–100) was observed in PANI/epoxy composites fabricated with the blending method; this means that the charge carriers were localized within the domains and could not hop to the adjacent regions. They also prepared a PANI–dodecylbenzene sulfonic acid (DBSA)/poly(acrylic acid) system with a reversed micelle method (Figure 3).[54] Briefly, PANI was synthesized via the emulsion polymerization of aniline (Ani.) monomers in an *n*-hexane/water system, and DBSA served as an emulsifier and a dopant during the PANI formation. Then, the freshly obtained PANI–DBSA solution was blended with a poly(acrylic acid) solution, which acted a suspension agent. In this system, when the PANI loading was lower than 6 wt %, a positive permittivity was observed. When the PANI loading was higher than 6 wt %, the permittivity became negative within the frequency range from 5.0×10^2 to 1.0×10^7 Hz. The obtained negative permittivity was a function of the PANI loading and the frequency.

Tanrıverdi et al.[55] prepared PANI/cobalt ferrite ($CoFeO_4$) nanocomposites, in which different permittivity values were obtained; this was dependent on the ferrite nanoparticle loadings. For the synthesized pure PANI, a very large negative permittivity (ca. 10^{-5} at low frequencies of 1–10 Hz) was obtained. With increasing ferrite nanoparticle loading, the negative permittivity gradually became positive and then fluctuated at negative values. The researchers thought that the negative permittivity might have been due to the large plasmon resonance conductivity at a relatively low frequency.[56] Interestingly, they also used a volume fraction average method and Maxwell equation to explain the mechanism of how the dielectric properties of the nanocomposites depended on the dielectric properties of the polymer and the host materials. The volume fraction average method was used to determine the effective dielectric constant (ε_{eff}), as described in eq. (7):[55]

$$\varepsilon_{eff} = \phi_1 \varepsilon_1 + \phi_2 \varepsilon_2 \tag{7}$$

where ϕ is the volume fraction of the constituents. The Maxwell equation is represented by eq. (8):[55]

$$\varepsilon_{eff} = \varepsilon_1 \frac{\varepsilon_2 + 2\varepsilon_1 - 2(1-\phi_1)(\varepsilon_1 - \varepsilon_2)}{\varepsilon_2 + 2\varepsilon_1 + 2(1-\phi_1)(\varepsilon_1 - \varepsilon_2)} \tag{8}$$

The fitting results show that the volume fraction model was more accurate than the Maxwell equation because of the large order of difference between the dielectric constants of $CoFeO_4$ ($\varepsilon' = 25$) and PANI ($\varepsilon' = -2 \times 10^5$).

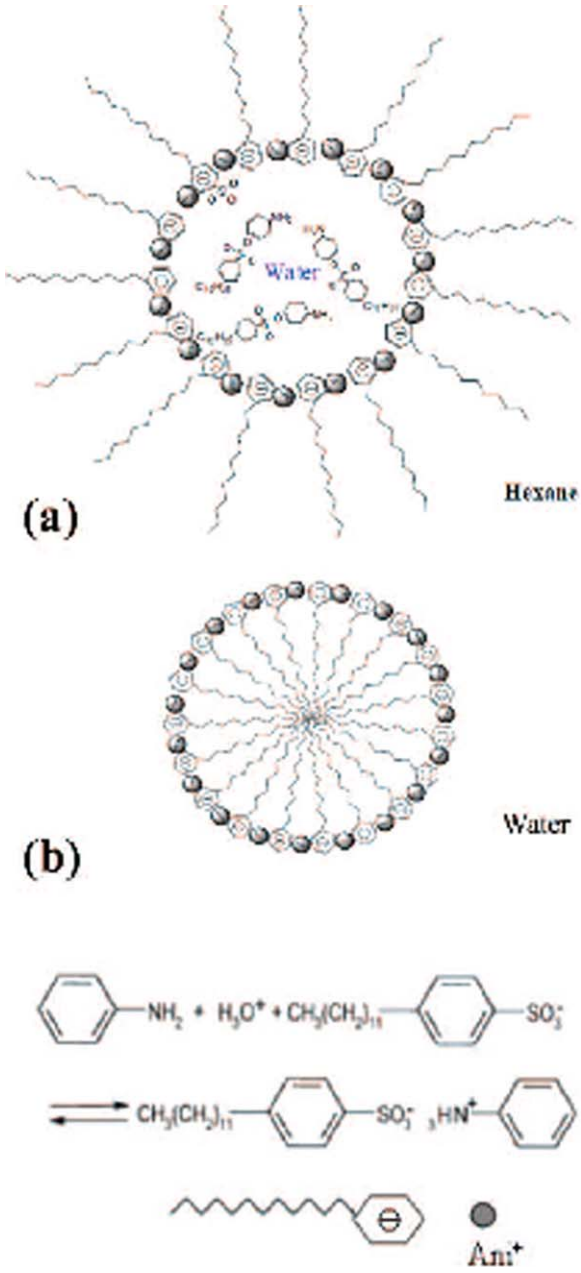

Figure 3. Schematic of the micellar structure: (a) regular micelle and (b) reversed micelle. (Reprinted with permission from ref. 54. Copyright 2012 AIP Publishing.) [Color figure can be viewed in the online issue, which is available at wileyonlinelibrary.com.]

Recently, the permittivity values of PANI nanocomposites reinforced with different nanofillers synthesized by a surface-initiated polymerization method have been reported.[9,11,57–59] In tungsten oxide (WO_3)/PANI nanocomposites,[9] the permittivity could be easily tuned by changing the loading and morphology of the nanofillers. The ε' and ε'' transition from negative to positive was observed in synthesized samples (Figure 4). This switching frequency, at which the permittivity (both for ε' and ε'') switched from negative to positive, increased with increasing

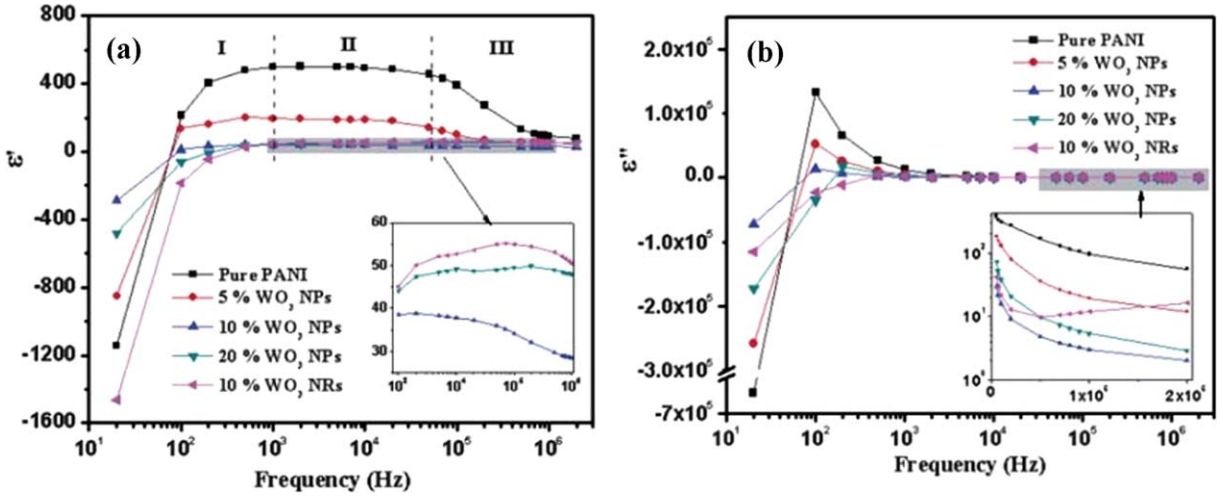

Figure 4. (a) ε' and (b) ε'' values of pure PANI and its WO_3 nanocomposites as a function of frequency. NPs represents nanoparticles and NRs are nanorods. (Reproduced with permission from ref. 9. Copyright 2011 RSC Publications.) [Color figure can be viewed in the online issue, which is available at wileyonlinelibrary.com.]

WO_3 nanoparticle loading. ε' of the WO_3 nanorods/PANI nanocomposites was lower than that of the WO_3 nanoparticles/PANI nanocomposites in a low frequency range (20–400 Hz) because of the larger aspect ratio of the nanorods. In Al_2O_3/PANI nanocomposites,[57] a positive permittivity was obtained within the measured frequency range (20–2 × 10^6 Hz) and was strongly related to both the morphology and the dispersion quality of the nanofillers. In the magnetite (Fe_3O_4)/PANI nanocomposites,[11] a negative permittivity was observed in all of the samples within the whole frequency range (20–2 × 10^6 Hz) at room temperature; this indicated the weak localization behavior and the intrinsic metallic nature of PANI (Figure 5). Meanwhile, a percolation threshold was observed in Fe_3O_4/PANI nanocomposites with a Fe_3O_4 nanoparticle loading of 16.67 wt %; this provided the highest level of charge delocalization for the PANI. As the Fe_3O_4 loading was increased further, the charge transport in the PANI was interrupted; this limited the charge delocalization. In the PANI nanocomposites with different carbon nanostructures,[58] the effects of different carbon nanostructures, including graphene, carbon nanotubes (CNTs), and CNFs on the permittivity of the PANI matrix were studied. Specifically, the researchers found that the interfacial properties, which were determined by the nanofiller morphology, dimensions, surface functionality, and intrinsic physicochemical nature of the nanofillers, affected the permittivity in different ways. Permittivity switching from negative to positive at certain frequencies was observed in all of the synthesized PANI nanocomposites (Figure 6). This transition frequency increased with increasing graphene loading from 0.1 to 3.0 wt % and then slightly decreased as the graphene loading increased to 5.0 wt % [Figure 6(b)]. As shown in Figure 6(e), the switching frequency of the nanocomposites filled with CNTs and CNFs was higher than that of the nanocomposites filled with graphene because of the charge delocalization at the interface, which arose from the excellent interfacial interaction between the PANI matrix and CNTs or CNFs. The appearance of the peak in the dielectric loss (tan δ) curve was due to the resonance effect, in which frequency of the system tended to oscillate with greater amplitude than others, especially for the negative permittivity values.[60] In barium titanate ($BaTiO_3$)/PANI nanocomposites,[59] a negative ε' for nanocomposites synthesized with a surface-initiated polymerization method (a chemical process) was also observed within the measured frequency range (from 20 to 2 × 10^6 Hz). However, $BaTiO_3$/PANI nanocomposites prepared with a physical mixture of $BaTiO_3$ and pure PANI showed a positive ε'; this was attributed to the storage of charges arising from the ferroelectric nature of $BaTiO_3$.[61]

Kavas et al.[62] synthesized PANI–Fe_3O_4 nanocomposites with an ionic liquid [1-butyl-3-methyl-imidazolium bromide (BMI MBr)] via *in situ* polymerization with cetyl trimethylammonium bromide as a surfactant. BMIMBr was reported to have an important effect on the ε' of the PANI–Fe_3O_4 nanocomposites, which had negative values in the low-frequency and low-temperature region. However, ε' was always positive within the

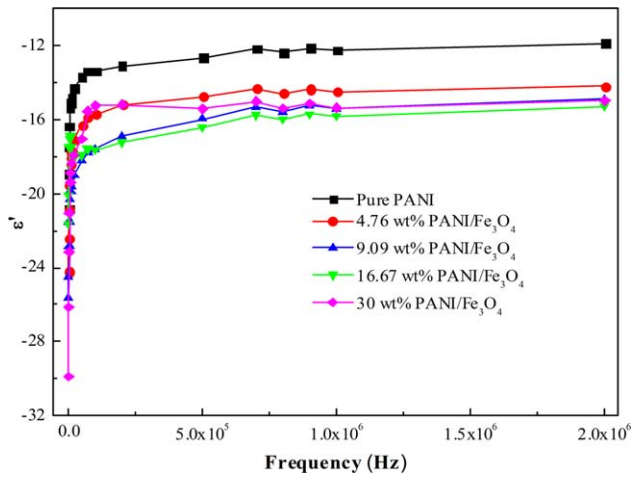

Figure 5. ε' as a function of the frequency for pure PANI and its Fe_3O_4 nanocomposites. (Reproduced with permission from ref. 11. Copyright 2012 Elsevier Publications.) [Color figure can be viewed in the online issue, which is available at wileyonlinelibrary.com.]

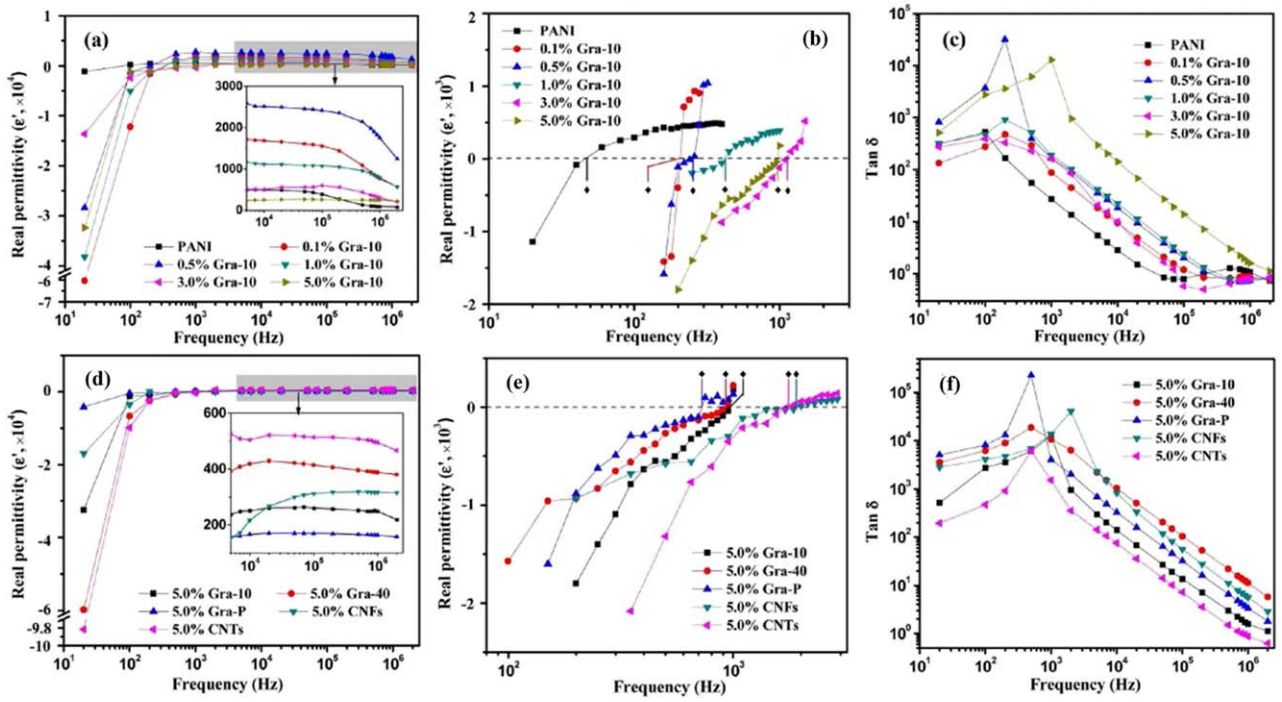

Figure 6. Frequency-dependent (a) ε' from 20 to 2×10^6 Hz, (b) ε' from 200 to 10^4 Hz, and (c) tan δ for pure PANI and the PANI nanocomposites with different loadings of Gra-10 (graphene) and (d) ε' from 20 to 2×10^6 Hz, (e) ε' from 200 to 10^4 Hz, and (f) tan δ of the PANI nanocomposites with the same loading of different carbon nanostructures. Gra-10, Gra-40, and Gra-P represent the different types of graphene. (Reproduced with permission from ref. [58]. Copyright 2012 ACS Publications.) [Color figure can be viewed in the online issue, which is available at wileyonlinelibrary.com.]

whole frequency range for the PANI–Fe_3O_4 nanocomposites without BMIMBr.

CONCLUSIONS AND PERSPECTIVES

In this article, the fundamentals of negative permittivity in materials have been critically examined. Current research reports on PANI and its nanocomposites with negative permittivity values are presented in detail. The reasons behind the negative permittivity have been provided as well. The synthesis of PANI nanostructures and nanocomposites with negative permittivities is an approach used to improve the material quality of polymer systems. This method could provide high-performance semiconducting and metallic polymers in plastic electronics, which would significantly extend the applications of these metamaterials.[38] However, how to use the volume fraction of the nanofillers in the PANI matrix to obtain a controllable negative permittivity for different applications at certain frequencies, especially high frequencies, is still a challenge. Meanwhile, because the negative permittivity of PANI nanostructures and nanocomposites is strongly related to the continuous conductive path, approaches for preparing highly conductive PANI nanostructures and nanocomposites with negative permittivities in a certain frequency range are a trend for the future research.

ACKNOWLEDGMENTS

This work was financially supported by National Science Foundation—Nanomanufacturing under the EArly-concept Grants for Exploratory Research (EAGER) program (CMMI 13-14486), Nanoscale Interdisciplinary Research Team and Materials Processing and Manufacturing (CMMI 10-30755), and Chemical and Biological Separations under the EAGER program (CBET 11-37441). One of the authors (H.G.) acknowledges support from the China Scholarship Council program.

REFERENCES

1. Valentine, J.; Zhang, S.; Zentgraf, T.; Ulin-Avila, E.; Genov, D. A.; Bartal, G.; Zhang, X. *Nature* **2008**, *455*, 376.
2. Shalaev, V. M. *Nat. Photonics* **2007**, *1*, 41.
3. Ziolkowski, R. W.; Heyman, E. *Phys. Rev. E* **2001**, *64*, 056625.
4. Capolino, F. In Theory and Phenomena of Metamaterials; CRC: Boca Raton, FL, **2009**.
5. Veselago, V. G. *Phys. Usp.* **1968**, *10*, 509.
6. Smith, D. R.; Pendry, J. B.; Wiltshire, M. C. K. *Science* **2004**, *305*, 788.
7. Yao, J.; Liu, Z.; Liu, Y.; Wang, Y.; Sun, C.; Bartal, G.; Stacy, A. M.; Zhang, X. *Science* **2008**, *321*, 930.
8. Li, B.; Sui, G.; Zhong, W.-H. *Adv. Mater.* **2009**, *21*, 4176.
9. Zhu, J.; Wei, S.; Zhang, L.; Mao, Y.; Ryu, J.; Karki, A. B.; Young, D. P.; Guo, Z. *J. Mater. Chem.* **2011**, *21*, 342.
10. Zhu, J.; Wei, S.; Zhang, L.; Mao, Y.; Ryu, J.; Mavinakuli, P.; Karki, A. B.; Young, D. P.; Guo, Z. *J. Phys. Chem. C* **2010**, *114*, 16335.
11. Gu, H.; Huang, Y.; Zhang, X.; Wang, Q.; Zhu, J.; Shao, L.; Haldolaarachchige, N.; Young, D. P.; Wei, S.; Guo, Z. *Polymer* **2012**, *53*, 801.

12. Wei, S.; Mavinakuli, P.; Wang, Q.; Chen, D.; Asapu, R.; Mao, Y.; Haldolaarachchige, N.; Young, D.; Guo, Z. *J. Electrochem. Soc.* **2011**, *158*, K205.
13. Zhu, J.; Zhang, X.; Haldolaarachchige, N.; Wang, Q.; Luo, Z.; Ryu, J.; Young, D. P.; Wei, S.; Guo, Z. *J. Mater. Chem.* **2012**, *22*, 4996.
14. Zhu, J.; Wei, S.; Ryu, J.; Guo, Z. *J. Phys. Chem. C* **2011**, *115*, 13215.
15. Liu, C. D.; Lee, S. N.; Ho, C. H.; Han, J. L.; Hsieh, K. *J. Phys. Chem. C* **2008**, *112*, 15956.
16. Zhu, J.; Wei, S.; Haldolaarachchige, N.; He, J.; Young, D. P.; Guo, Z. *Nanoscale* **2012**, *4*, 152.
17. Zhu, J.; Luo, Z.; Wu, S.; Haldolaarachchige, N.; Young, D. P.; Wei, S.; Guo, Z. *J. Mater. Chem.* **2012**, *22*, 835.
18. Gu, H.; Tadakamalla, S.; Huang, Y.; Colorado, H. A.; Luo, Z.; Haldolaarachchige, N.; Young, D. P.; Wei, S.; Guo, Z. *Am. Chem. Soc. Appl. Mater. Interfaces* **2012**, *4*, 5613.
19. Gu, H.; Tadakamalla, S.; Zhang, X.; Huang, Y.-D.; Jiang, Y.; Colorado, H. A.; Luo, Z.; Wei, S.; Guo, Z. *J. Mater. Chem.C* **2012**, *1*, 729.
20. Zhang, X.; He, Q.; Gu, H.; Colorado, H. A.; Wei, S.; Guo, Z. *Am. Chem. Soc. Appl. Mater. Interfaces* **2012**, *5*, 898.
21. Zhang, X.; He, Q.; Gu, H.; Wei, S.; Guo, Z. *J. Mater. Chem. C* **2013**, *1*, 2886.
22. Dhawan, S. K.; Singh, N.; Rodrigues, D. *Sci. Technol. Adv. Mater.* **2003**, *4*, 105.
23. Guo, J.; Gu, H.; Wei, H.; Zhang, Q.; Haldolaarachchige, N.; Li, Y.; Young, D. P.; Wei, S.; Guo, Z. *J. Phys. Chem. C,* **2013**, *117*, 10191.
24. Wei, H.; Yan, X.; Wu, S.; Luo, Z.; Wei, S.; Guo, Z. *J. Phys. Chem. C* **2012**, *116*, 25052.
25. Zhu, J.; Chen, M.; Qu, H.; Zhang, X.; Wei, H.; Luo, Z.; Colorado, H. A.; Wei, S.; Guo, Z. *Polymer* **2012**, *53*, 5953.
26. Gu, H.; Guo, J.; We, H.; Huang, Y.; Zhao, C.; Li, Y.; Wu, Q.; Haldolaarachchige, N.; Young, D. P.; Wei, S.; Guo, Z. *RSC Adv.* **2012**, DOI:10.1039/C1033CP50698C.
27. Gonçalves, G.; Baldissera, A.; Rodrigues, L.; Martini, E.; Ferreira, C. *Synth. Met.* **2011**, *161*, 313.
28. Choi, M.-R.; Woo, S.-H.; Han, T.-H.; Lim, K.-G.; Min, S.-Y.; Yun, W. M.; Kwon, O. K.; Park, C. E.; Kim, K.-D.; Shin, H.-K.; Kim, M.-S.; Noh, T.; Park, J. H.; Shin, K.-H.; Jang, J.; Lee, T.-W. *ChemSusChem* **2011**, *4*, 363.
29. Wei, H.; Zhu, J.; Wu, S.; Wei, S.; Guo, Z. *Polymer* **2013**, *54*, 1820.
30. Gu, H.; Rapole, S. B.; Sharma, J.; Huang, Y.; Cao, D.; Colorado, H. A.; Luo, Z.; Haldolaarachchige, N.; Young, D. P.; Walters, B.; Wei, S.; Guo, Z. *RSC Adv.* **2012**, *2*, 11007.
31. Mike, J. F.; Lutkenhaus, J. L. *J. Polym. Sci. Part B: Polym. Phys.* **2013**, *51*, 468.
32. Bagheri, H.; Ayazi, Z.; Naderi, M. *Anal. Chim. Acta* **2013**, *767*, 1.
33. Aneli, J.; Zaikov, G.; Mukbaniani, O. *Mol. Cryst. Liq. Cryst. Sci.* **2012**, *554*, 167.
34. Liu, Y. D.; Park, B. J.; Kim, Y. H.; Choi, H. J. *J. Mater. Chem.* **2011**, *21*, 17396.
35. Ramakrishna, S. A.; Grzegorczyk, T. M. In Physics and Applications of Negative Refractive Index Materials; SPIE: Boca Raton, FL, **2009**; p 19.
36. McMahon, J. M.; Gray, S. K.; Schatz, G. C. *Phys. Rev. Lett.* **2009**, *103*, 097403.
37. Rashidi-Huyeh, M.; Palpant, B. *Phys. Rev. B* **2006**, *74*, 075405.
38. Lee, K.; Cho, S.; Park, S. H.; Heeger, A. J.; Lee, C. W.; Lee, S. H. *Nature* **2006**, *44*, 65.
39. MacDiarmid, A. G.; Manohar, S. K.; Masters, J. G.; Sun, Y.; Weiss, H.; Epstein, A. *J. Synth. Met.* **1991**, *41*, 621.
40. Ogoshi, T.; Hasegawa, Y.; Aoki, T.; Ishimori, Y.; Inagi, S.; Yamagishi, T.-A. *Macromolecules* **2011**, *44*, 7639.
41. Bhadra, S.; Khastgir, D.; Singha, N. K.; Lee, J. H. *Prog. Polym. Sci.* **2009**, *34*, 783.
42. Tung, N. T.; Lee, H.; Song, Y.; Nghia, N. D.; Sohn, D. *Synth. Met.* **2010**, *160*, 1303.
43. Nath, C.; Kumar, A. *J. Appl. Phys.* **2012**, *112*, 093704.
44. Nalwa, H. S. Handbook of Organic Conductive Molecules and Polymers: Conductive Polymers: Spectroscopy and Physical Properties; Wiley: Hoboken, New Jersey, USA, **1997**; p 368.
45. Joo, J.; Oh, E. J.; Min, G.; MacDiarmid, A. G.; Epstein, A. *J. Synth. Met.* **1995**, *69*, 251.
46. Prigodin, V. N.; Epstein, A. *J. Synth. Met.* **2002**, *125*, 43.
47. Wang, Z. H.; Li, C.; Scherr, E. M.; MacDiarmid, A. G.; Epstein, A. *J. Phys. Rev. Lett.* **1991**, *66*, 1745.
48. Wang, Y. Z.; Joo, J.; Hsu, C. H.; Epstein, A. *J. Synth. Met.* **1995**, *69*, 267.
49. Gu, H.; Guo, J.; Zhang, X.; He, Q.; Huang, Y.; Colorado, H. A.; Haldolaarachchige, N. S.; Xin, H. L.; Young, D. P.; Wei, S.; Guo, Z. *J. Phys. Chem. C* **2013**, *117*, 6426.
50. Phang, S.-W.; Hino, T.; Abdullah, M. H.; Kuramoto, N. *Mater. Chem. Phys.* **2007**, *104*, 327.
51. Zhang, X.; Zhu, J.; Haldolaarachchige, N.; Ryu, J.; Young, D. P.; Wei, S.; Guo, Z. *Polymer* **2012**, *53*, 2109.
52. Pillalamarri, S. K.; Blum, F. D.; Tokuhiro, A. T.; Bertino, M. F. *Chem. Mater.* **2005**, *17*, 5941.
53. Phang, S. W.; Tadokoro, M.; Watanabe, J.; Kuramoto, N. *Curr. Appl. Phys.* **2008**, *8*, 391.
54. Hsieh, C.-H.; Lee, A.-H.; Liu, C.-D.; Han, J.-L.; Hsieh, K.-H.; Lee, S.-N. *AIP Adv.* **2012**, *2*, 012127.
55. Tanrıverdi, E.; Uzumcu, A.; Kavas, H.; Demir, A.; Baykal, A. *Nano-Micro Lett.* **2011**, *3*, 99.
56. Legros, F.; Fourrier-Lamer, A. *Mater. Res. Bull.* **1984**, *19*, 1109.
57. Zhu, J.; Wei, S.; Zhang, L.; Mao, Y.; Ryu, J.; Haldolaarachige, N.; Young, D. P.; Guo, Z. *J. Mater. Chem.* **2011**, *21*, 3952.
58. Zhu, J.; Gu, H.; Luo, Z.; Haldolaarachige, N.; Young, D. P.; Wei, S.; Guo, Z. *Langmuir* **2012**, *28*, 10246.
59. Zhang, X.; Wei, S.; Haldolaarachchige, N.; Colorado, H. A.; Luo, Z.; Young, D. P.; Guo, Z. *J. Phys. Chem. C* **2012**, *116*, 15731.
60. Fredkin, D.; Mayergoyz, I. *Phys. Rev. Lett.* **2003**, *91*, 253902.
61. Patil, R. C.; Sushama Pethkar, S. R.; Vijaymohanan, K. *J. Mater. Res.* **2001**, *16*, 1982.
62. Kavas, H.; Günay, M.; Baykal, A.; Toprak, M. S.; Sozeri, H.; Aktaş, B. *J. Inorg. Organomet. Polym.* **2012**, *1*.